

## WATER AVAILABILITY SHAPES EDAPHIC AND LITHIC CYANOBACTERIAL COMMUNITIES IN THE ATACAMA DESERT<sup>1</sup>

Patrick Jung<sup>2</sup> , Michael Schermer, Laura Briegel-Williams

Plant Ecology and Systematics, University of Kaiserslautern, Erwin-Schrödinger-Straße 13, 67663 Kaiserslautern, Germany

Karen Baumann, Peter Leinweber

Faculty of Agricultural and Environmental Science, Soil Science, University of Rostock, Justus-von-Liebig-Weg 6, 18051 Rostock, Germany

Ulf Karsten 

Applied Ecology and Phycology, Institute of Biological Sciences, University of Rostock, Albert-Einstein-Straße 3, 18059 Rostock, Germany

Lukas Lehnert, Sebastian Achilles, Jörg Bendix

Faculty of Geography, Philipps-University of Marburg, Deutschhausstraße 10, 35037 Marburg, Germany

and Burkhard Büdel

Plant Ecology and Systematics, University of Kaiserslautern, Erwin-Schrödinger-Straße 13, 67663 Kaiserslautern, Germany

In the Atacama Desert, cyanobacteria grow on various substrates such as soils (edaphic) and quartz or granitoid stones (lithic). Both edaphic and lithic cyanobacterial communities have been described but no comparison between both communities of the same locality has yet been undertaken. In the present study, we compared both cyanobacterial communities along a precipitation gradient ranging from the arid National Park Pan de Azúcar (PA), which resembles a large fog oasis in the Atacama Desert extending to the semiarid Santa Gracia Natural Reserve (SG) further south, as well as along a precipitation gradient within PA. Various microscopic techniques, as well as culturing and partial 16S rRNA sequencing, were applied to identify 21 cyanobacterial species; the diversity was found to decline as precipitation levels decreased. Additionally, under increasing xeric stress, lithic community species composition showed higher divergence from the surrounding edaphic community, resulting in indigenous hypolithic and chasmoendolithic cyanobacterial communities. We conclude that rain and fog water, respectively, cause contrasting trends regarding cyanobacterial species richness in the edaphic and lithic microhabitats.

**Key index words:** 16S rRNA; Atacama Desert; Chasmoendolithic; Coastal Cordillera; cyanobacteria; hypolithic; quartz

**Abbreviations:** a.s.l., above sea level; C<sub>inorg</sub>, inorganic carbon; CLSM, confocal laser scanning microscopy; C<sub>org</sub>, organic carbon; CTAB, cetyltrimethylammoniumbromide; C<sub>t</sub>, total carbon; EC, electrical conductivity; EPS, extracellular polysaccharides; mg, milligram; nMDS, nonmetric multidimensional scaling; N<sub>t</sub>, total nitrogen; PA, Pan de Azúcar; P<sub>t</sub>, total phosphorus; SG, Santa Gracia; S<sub>t</sub>, total sulfur

Cyanobacteria in the Atacama Desert can be found as soil-inhabiting (edaphic) as well as stone-inhabiting (lithic) communities. Schulze-Makuch et al. (2018) reported edaphic communities from soils of the hyperarid core of the Atacama Desert where they are only temporarily active. Lithic communities develop in cracks and fissures of porous and nonporous rocky substrates (chasmoendolithic; Diruggiero et al. 2013) or as biofilms under, for example, translucent quartz stones (hypolithic; Azúa-Bustos et al. 2011).

In harsh environments, such as hot or polar deserts, these quartz stones function as refugia and “diversity oases” by providing habitat to more than 60 different species, including cyanobacteria, heterotrophic bacteria, archaea, and green algae (Pointing et al. 2009, Azúa-Bustos et al. 2012). Therefore, cryptic modes of colonization (hypolithic, chasmoendolithic) represent a stress avoidance mechanism

<sup>1</sup>Received 10 September 2018. Accepted 5 July 2019. First Published Online 4 August 2019. Published Online 9 September 2019, Wiley Online Library (wileyonlinelibrary.com).

<sup>2</sup>Author for correspondence: e-mail patrick\_jung90@web.de. Editorial Responsibility: D. Lindell (Associate Editor)

where the habitat beneath the substrate surface provides stability as well as buffering from extremes in temperature, water availability, and UV radiation (Wierzchos et al. 2013). This type of adaptive mechanism is well known for organisms common in drylands, such as cyanobacteria that require a microbial or substrate “cabana” with multiple protective characters, this has been described as the “cabana strategy” (Pointing and Belnap 2012). Tracy et al. (2010) found that in Northern Australia hypolithic cyanobacteria can be active for about 75 days during a year using this life strategy. Hypolithic cyanobacterial communities can colonize up to 80% of all stones in a location, thriving on fog as the main regular source of water (Azúa-Bustos et al. 2011). Quartz stones from the Atacama Desert, for example, have a higher thermal conductivity than the surrounding soil resulting in lower daytime temperatures at the quartz–soil interface, creating a microenvironment which favors water condensation and thus enables colonization by hypolithic species (Azúa-Bustos et al. 2011). However, it remains unknown how water availability, including fog water input, affects edaphic and lithic cyanobacterial communities in the Atacama Desert. Warren-Rhodes et al. (2007) suggested that the efficiency of moisture capture from fog by surface rocks increased with increasing rock size, which was supported by Azúa-Bustos et al. (2011), who found high colonization rates of quartz stones with a weight greater than 20 g. Although predicted productivity rates of the hypolithic cyanobacterial communities of approximately  $1 \text{ g C} \cdot \text{m}^{-2} \cdot \text{y}^{-1}$  are low, hypolithic cyanobacterial biomass production provides an important food source for grazing nematodes and protozoans, therefore, providing the basis for the vitality of a whole ecosystem in extreme environments (Thomas 2005, De los Ríos et al. 2014).

Lithic locations have been described as refugia for communities from virtually all deserts of the world (Vogel 1955, Rundel et al. 1990, Gorbushina 2007, Warren-Rhodes et al. 2007, Adriaenssens et al. 2015, Le et al. 2016, Christian et al. 2017), but less attention has been paid to the comprehensive edaphic cyanobacterial diversity present in soils of the same sites. Except for a few studies, comparisons of edaphic and lithic communities from the same location have rarely been conducted (Pointing et al. 2009, Van Goethem et al. 2016). It remains unclear whether lithic microenvironments, with their protective character, represent a true “oasis” for all cyanobacterial species found in the soil or if there are pronounced microhabitat-related communities.

The aim of this study was to elucidate for the first time the relationship between adjacent edaphic and lithic cyanobacterial communities and describe differences in species richness and composition depending on environmental parameters in a large fog oasis of the Atacama Desert. In the present study, we investigated corresponding microhabitats along a North–South and West–East precipitation gradient in

the southern edge of the Atacama Desert including unstudied areas. We hypothesized that (i) cyanobacterial species richness in edaphic as well as lithic habitats decreases with decreasing water availability, since only specialized species are expected to cope with high xeric stress. Additionally, it was hypothesized that (ii) the divergence of soil- (edaphic) and stone (lithic)-inhabiting cyanobacterial communities increases with decreasing water availability because quartz stones provide a protective “cabana.” We evaluated these hypotheses using a polyphasic approach including culturing, partial sequencing of the 16S rRNA, and various microscopic techniques applied to soil and biofilms from different hypo- and chasmoendolithic substrates to generate an in-depth overview of the dominant cyanobacterial taxa.

## MATERIALS AND METHODS

**Sampling site description.** Soil substrate, as well as biofilms from stones, were collected at four different sites in Chile (Fig. 1): three sites (forming the West–East precipitation gradient) were situated along the Coastal Cordillera in the National Park of Pan de Azúcar (PA; arid site) in the Atacama Desert (Fig. 1b) and one site was at the Santa Gracia Natural Reserve (SG; semiarid site;  $29^{\circ}45'33'' \text{ S}$ ;  $71^{\circ}09'57'' \text{ W}$ ; 704 m a.s.l.; Fig. 1f), 500 km south of PA (N–S precipitation gradient). In both areas, cacti and *Euphorbia* shrubs were present and allowed the settlement of animals, such as Guanacos and foxes (Bernhard et al. 2018). At PA, the West–East precipitation gradient ranged from the top hills close to the coast (PA ridge;  $25^{\circ}59'03'' \text{ S}$ ,  $70^{\circ}36'55'' \text{ W}$ ; 764 m a.s.l.; Fig. 1c) over a transect 2.5 km further inland (PA grit;  $25^{\circ}58'24'' \text{ S}$ ;  $70^{\circ}36'56'' \text{ W}$ ; 667 m a.s.l.; Fig. 1d) to the beginning of the core zone of the desert (PA core;  $26^{\circ}06'39'' \text{ S}$ ;  $70^{\circ}32'54'' \text{ W}$ ; 409 m a.s.l.; Fig. 1e) 15 km from the coast. This gradient was accompanied by changing soil structures comprised of loamy sand at PA ridge, quartz and granitic grit at PA grit, as well as quartz grit and granitic stones at PA core. Liquid water supply by dew and fog plays a major role at the National Park PA and as reported in Lehnert et al. (2018) the latter is blown inland from the coast. Quartz stones of various sizes with hypolithic cyanobacteria were found randomly distributed over the ground at PA ridge, PA grit, PA core and SG. In addition, limestones colonized by hypolithic cyanobacteria and granitic stones with chasmoendolithic cyanobacteria growing in cracks were found at PA core. The N–S precipitation gradient was represented by PA and SG, which have differing climates, for the most part, due to mean annual rainfall amounts of 15 and 83  $\text{mm} \cdot \text{y}^{-1}$ , respectively (Baumann et al. 2018).

**Precipitation measurement.** Three automatic weather stations were installed in March 2016 at PA ridge and PA core, as well as at SG, as described in Lehnert et al. (2018). The stations were equipped with standard sensors measuring rainfall with a rain gauge, temperature, relative humidity, solar radiation, and soil temperature. Fog water fluxes were measured with a cylindrical fog collector (“harp”-type) at PA ridge and SG stations designed according to Falconer and Falconer (1980). Measuring intervals were set to 5 min. Rainfall was recorded from January 2017 to December 2017, which was partly influenced by El Niño-like conditions where positive sea surface temperature anomalies off the coast generated cut-off lows bringing unusual rain events to this arid area (Bozkurt et al. 2016).

**Soil parameters.** For soil analyses, three replicates of barren substrate were taken from the top 5 to 10 mm of each site.

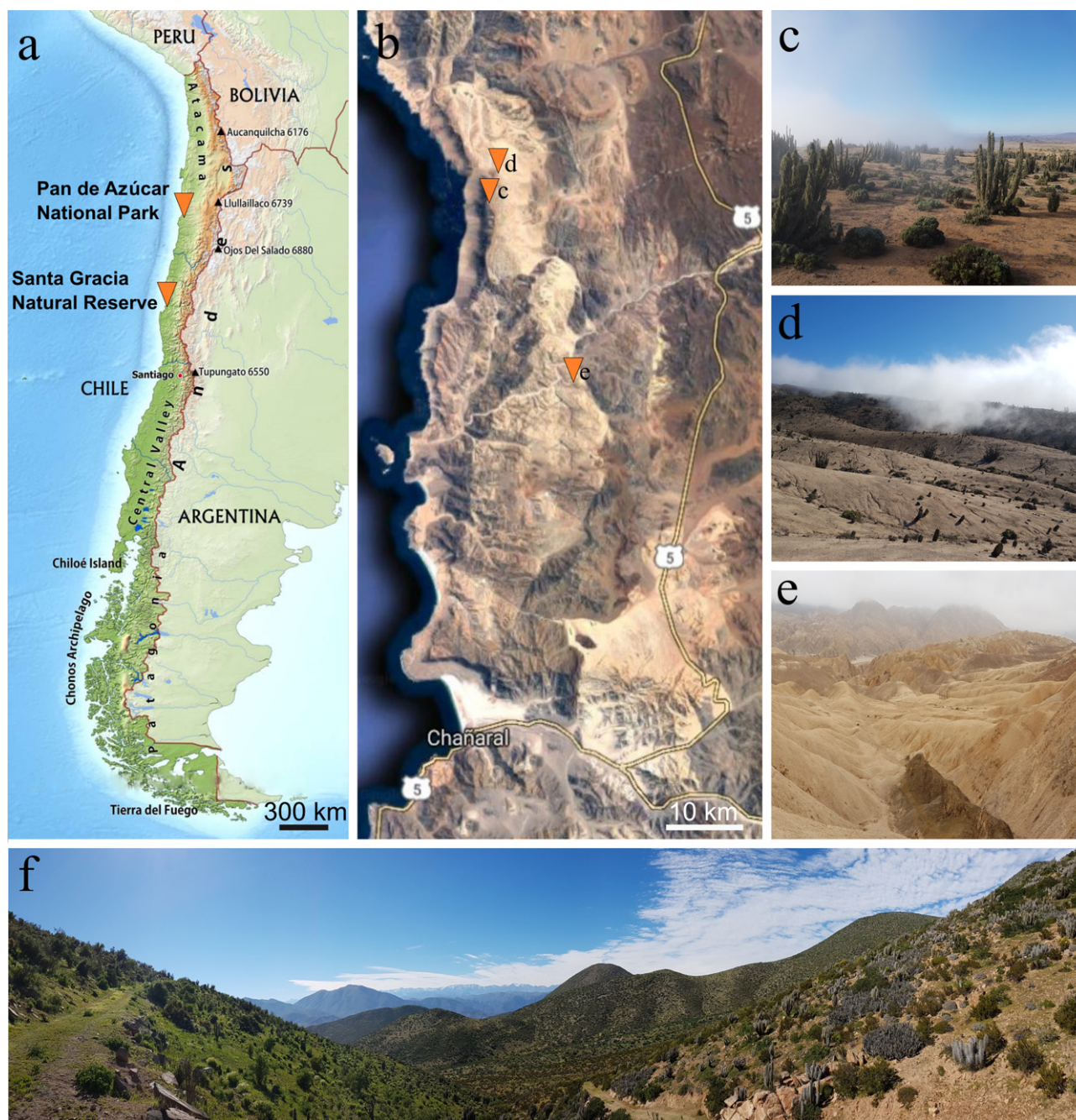


FIG. 1. Sampling sites. (a) Map of Chile showing the two sites studied, Pan de Azúcar National Park and Santa Gracia Natural Reserve. (b) Map of the Pan de Azúcar National Park with the sites PA ridge (c), PA grit at (d), and PA core (e). (f) View of the Santa Gracia Natural Reserve sampling site. Images were taken during the local winter season. [Color figure can be viewed at [wileyonlinelibrary.com](http://wileyonlinelibrary.com)]

The pH ( $H_2O$ , 1:2.5 w:v) and electrical conductivity (EC, 1:5 w:v) of air-dried soil were determined by standard procedures as described by Blume et al. (2011). For total element analyses, air-dried substrate was ground to  $<0.5$  mm particle size. Total C, N, and S ( $C_t$ ,  $N_t$ ,  $S_t$ ) were measured using a Vario EL elemental analyzer (Elementar Analysensysteme, Hanau, Germany). Inorganic carbon ( $C_{inorg}$ ) was determined by a Scheibler calcimeter and organic carbon ( $C_{org}$ ) was calculated from the differences (Blume et al. 2011). Total Al, Ca, Fe, K, Mg, Mn, P, and Zn were extracted from 0.5 g of substrate by microwave-assisted digestion with Aqua regia solution (3:1

hypochloric acid:nitric acid) (Chen and Ma 2001; ISO standard 11466) and their concentration was subsequently determined by inductively coupled plasma-optical emission spectroscopy.

**Cyanobacteria sampling.** At each sampling site, seven stones of the dominant type (quartz at PA ridge, PA grit, PA core, SG; limestone at PA core; granite at PA core) larger than 5 cm (or  $>15$  g) were randomly collected. Hypolithic cyanobacterial biofilms from the bottom or the edges of five stones were completely removed with a sterile scalpel and stored in falcon tubes. Chasmoendolithic cyanobacteria were

scratched off naturally occurring cracks after breaking the granite stones. The additional two stones were used for direct microscopic observations by various techniques. For investigation of the edaphic cyanobacterial community, soil samples were taken by pressing five sterile 9 cm diameter Petri dishes randomly into the soil in close vicinity (within 2 m) to the collected stones at each sampling site. All samples were collected in July 2017, shipped air-dry and stored frozen in the laboratory until the beginning of investigations 2 weeks later. Experience has shown that this treatment does not affect species diversity at microscopic or DNA levels.

**Enrichment cultures and isolation.** Enrichment cultures from soil material and biofilms were prepared as described in Jung et al. (2018b) on solidified basal medium (BBM; Bischof and Bold 1963) and solidified BG11 medium (Stanier et al. 1971). The enrichment cultures were kept in a culture cabinet at 15–17°C under a light/dark regime of 14:10 h at a photon fluence rate of 20–50  $\mu\text{mol photons} \cdot \text{m}^{-2} \cdot \text{s}^{-1}$  as described in Langhans et al. (2009), for at least 4 weeks. The cultures were inspected twice a week for the appearance of cyanobacteria and colonies were transferred with a sterile metal needle to new BG11 medium agar plates. This was repeated until unialgal cultures were established. The growth of the colonies was frequently monitored, and several subcultures were generated by further serial transfers under sterile conditions, until contamination with other cyanobacteria, green algae, or fungi was eradicated and unialgal stock isolates could be established.

**Microscopic investigations.** Scanning electron microscopy (FEI) and CLSM were applied directly to air-dried and wet biofilms attached to the stones in order to present an in situ snapshot of the undisturbed cyanobacterial community. Air-dried biofilms were expected to show the interaction between the particles of the substrate and the cyanobacteria, while the wet biofilms reflected the proportion of conspicuous cyanobacterial species more appropriately. Additionally, biofilms were scraped from the quartz stones and dissolved in water. A droplet of water was transferred to an objective slide and investigated by light microscopy to directly identify the species of the biofilm. The biofilm organisms were cultivated on agar plates and isolates were prepared and studied by light microscopy.

Images of air-dried biofilms were obtained with an FEI Helios NanoLab 650 microscope (FEI) without cryopreparation. The different microscopic methods were applied to all lithic samples and one sample is shown for colonized quartz stones from PA ridge (Fig. 2).

Wet biofilms attached to quartz stones were directly visualized with a CLSM (LSM700, Carl Zeiss, Jena, Germany) equipped with diode lasers as described in the study by Jung et al. (2018a). Photomultiplier parameters were adjusted to achieve the maximum signal from cyanobacteria, while simultaneously keeping the noise signals generated by quartz and adhering soil particles to a minimum. Their maximum projection was converted into 2-D pictures to give an overview of the in situ community.

Small proportions of cyanobacterial isolates from agar plates were transferred to a drop of water on an objective slide under a binocular stereoscope. Cyanobacterial strains were studied by light microscopy (Axioskop; Carl Zeiss) using oil immersion and a 630-fold magnification in combination with AxioVision software (Carl Zeiss) and appropriate taxonomic keys (Geitler 1932, Komárek and Anagnostidis 1998, 2005). Species identified by light microscopy or obtained sequences were displayed with their most recent species names (e.g., *Leptolyngbya badia* described by Johansen et al. 2011, = *Trichocoleus badius* redefined by Mühlsteinova et al. 2014).

**DNA extraction and PCR.** Total genomic DNA of cyanobacterial isolates was extracted using a cetrimonium bromide (CTAB) method followed by phenol–chloroform–isoamyl alcohol purification adapted for BSCs (Williams et al. 2017b). DNA was stored at -20°C until further processing. A nested PCR approach was chosen for a first PCR with the primer set 27F1 and 1494Rc followed by a subsequent second PCR with the primer set CYA361f and CYA785r for cyanobacteria (Mühling et al. 2008), but instead of 59°C, an annealing temperature of 61°C was applied. The obtained PCR products were cleaned by using the NucleoSpin® Gel and PCR Clean-up Kit. Cleaned PCR products were sequenced by Seq-It GmbH & Co. KG (Pfaffplatz 10, 67655 Kaiserslautern, Germany), the resulting sequences were submitted to the European Nucleotide Archive (ENA) and can be found under the project code PRJEB31521. They were compared with publicly available sequences in the National Center for Biotechnology Information (NCBI) database (<http://www.ncbi.nlm.nih.gov/>) using the Basic Local Alignment Search Tool for Nucleotides search function.

**Phylogenetic tree.** The 16S rRNA gene sequences were aligned using the ClustalW algorithm of Mega 7 (Kumar et al. 2016) and refined manually using conservation of secondary structure as a guide where necessary. The evolutionary history was inferred by using the maximum likelihood method based on the Jukes–Cantor model (Jukes et al. 1969), produced with Mega 7. The bootstrap consensus tree inferred from 500 replicates was taken to represent the evolutionary history of the taxa analyzed, rooted to *Gloeobacter violaceus* PCC 7421. A total of 389 bp was used as partial 16S rRNA gene sequence in the final dataset. The percentage of replicate trees in which the associated taxa clustered together in the bootstrap test is shown next to the branches. Initial trees for the heuristic search were obtained automatically by applying Neighbor-Joining and BioNJ algorithms to a matrix of pairwise distances estimated using the maximum composite likelihood approach, and then selecting the topology with a superior log likelihood value. All positions containing gaps and missing data were eliminated. Alternative maximum likelihood trees with bootstrap analyses using Paup 4.0b10 yielded similar results to trees made with Seaview 4.0 (data not shown).

**Statistics.** The soil parameters were not always found to conform to a normal distribution according to the Kolmogorov–Smirnov test, therefore, *F*-tests and heteroscedastic *t*-test were used to verify homogenous variances and analyze differences between sites, respectively. The effect of soil parameters on the alpha-diversity (richness) of the cyanobacteria was tested by Spearman's correlation. The similarities between edaphic and hypo-/chasmoidolithic cyanobacteria communities were visualized in a nonmetric multidimensional scaling (nMDS) plot. Plots with a 2D stress <0.2 are considered to provide a good representation of the overall structure of the communities. The effect of soil parameters on the Beta-diversity (community structures) was determined by PerManova (with adonis function in R [Anderson 2001]) using the Bray–Curtis dissimilarity index (Bray and Curtis 1957), including permutation test with 999 permutations. All statistical analyses were performed using R version 3.4.3 (R Development Core Team 2017). Unless otherwise noted, significant differences refer to  $P \leq 0.05$ .

## RESULTS

**Precipitation.** In total, 110 mm of precipitation (including fog water deposition) was recorded for PA ridge, 17 mm for PA core, and 120 mm for SG from January to December 2017, which was in part

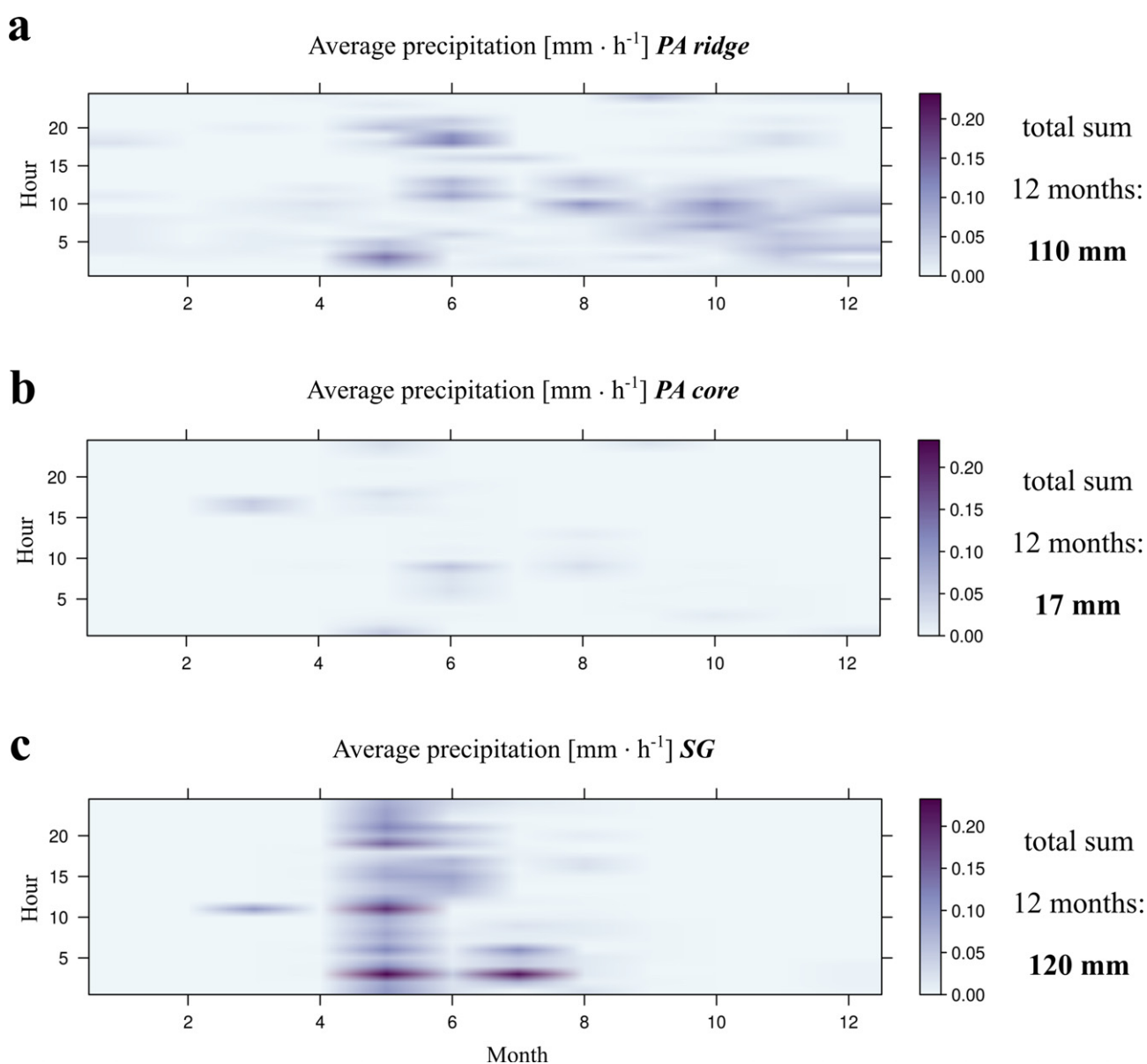


FIG. 2. Average precipitations between January and December of 2017. (a) PA ridge site, (b) PA Core site, and (c) SG site with their corresponding total sum measured during the record period of 1 year. [Color figure can be viewed at [wileyonlinelibrary.com](http://wileyonlinelibrary.com)]

TABLE 1. Sampling sites' soil parameters (mean values  $\pm$  SD,  $n = 3$ ). PA, Pan de Azucar; SG, Santa Gracia; small letters show significant differences between sites.

	$C_t$ ( $\text{g} \cdot \text{kg}^{-1}$ )	$C_{\text{inorg}}$ ( $\text{g} \cdot \text{kg}^{-1}$ )	$C_{\text{org}}$ ( $\text{g} \cdot \text{kg}^{-1}$ )	$N_t$ ( $\text{g} \cdot \text{kg}^{-1}$ )	$S_t$ ( $\text{g} \cdot \text{kg}^{-1}$ )	Al ( $\text{g} \cdot \text{kg}^{-1}$ )	Ca ( $\text{g} \cdot \text{kg}^{-1}$ )	Fe ( $\text{g} \cdot \text{kg}^{-1}$ )
PA ridge	$0.82 \pm 0.33$	$0.03 \pm 0.00$	$0.79 \pm 0.33$	$0.10 \pm 0.03$	$0.08 \pm 0.04$	$18.62 \pm 5.14^{\text{ab}}$	$1.78 \pm 0.82$	$37.84 \pm 1.71^{\text{b}}$
PA grit	$0.33 \pm 0.20$	$0.17 \pm 0.08$	$0.16 \pm 0.13$	$0.03 \pm 0.02$	$0.06 \pm 0.01$	$4.30 \pm 0.77^{\text{a}}$	$5.70 \pm 3.38$	$14.08 \pm 2.77^{\text{a}}$
PA core	$0.07 \pm 0.04$	$0.03 \pm 0.01$	$0.05 \pm 0.03$	$0.01 \pm 0.00$	$0.06 \pm 0.03$	$3.70 \pm 2.92^{\text{a}}$	$6.49 \pm 2.02$	$11.35 \pm 9.17^{\text{a}}$
SG <sup>cc</sup>	$0.57 \pm 0.18$	$0.06 \pm 0.06$	$0.52 \pm 0.22$	$0.06 \pm 0.02$	$0.03 \pm 0.01$	$10.03 \pm 0.95^{\text{b}}$	$5.28 \pm 1.15$	$38.66 \pm 5.70^{\text{b}}$

influenced by El Niño-like conditions (Fig. 2). Almost zero rainfall could be recorded from all sites during summer time between January and April and an intensive rain period occurred in May at SG (Fig. 2c).

**Soil parameters.** Soils of the sampled sites showed no significant differences regarding  $C_t$ , inorganic carbon ( $C_{inorg}$ ), organic carbon ( $C_{org}$ ),  $N_t$ ,  $S_t$ , calcium (Ca), magnesium (Mg), manganese (Mn) contents and EC (Table 1). The sites PA grit and PA core showed similar low concentrations of total aluminum (Al), iron (Fe), potassium (K), and  $P_t$  ranging from 3.7 to 4.3, 11 to 14, 1.7 to 1.9  $g \cdot kg^{-1}$ , and 185 to 261  $mg \cdot kg^{-1}$ , respectively. Similar high concentrations of total Al, Fe, and K were found at PA ridge and SG ranging from 10 to 19, 38 to 39, and 2 to 6  $g \cdot kg^{-1}$ , respectively. Soil pH was between 6.5 (PA ridge) and 8.1 (SG) and, thus, differed significantly between sites. According to Per-*Manova* calculations, soil parameters were not found to significantly influence the variance of the communities (data not shown).

**Image analysis.** To present an in situ snapshot of an undisturbed hypolithic cyanobacterial community, a biofilm attached to a quartz stone from PA ridge (Fig. 3, a and b) was investigated in detail with different microscopic techniques in an air-dry and wet state (Fig. 3, c and d). The biofilm contained a diverse community of cyanobacteria with single cells suggesting the presence of *Pleurocapsa* sp. as the most abundant growth form. In addition, filamentous morphologies suggest the presence of *Pseudophormidium* sp. and *Nostoc* sp. During in situ investigations of an air-dry state with the FEI microscope, a dense matrix of mineral particles, filamentous cyanobacteria (likely *Pseudophormidium* sp.), and undefined clumps were observed (Fig. 3c). Observations with CLSM of similar parts of the same stone in a wet state (Fig. 3d) showed the co-occurrence of filamentous (*Pseudophormidium* sp.) and coccoidal cyanobacteria (*Pleurocapsa minor*). These strong differences in the presence of *P. minor* between wet and air-dried samples were found for all quartz stones studied. In contrast to cyanobacteria, green algae always played a minor role in all lithic biofilms.

**Community composition.** A total of 21 species across all sites and substrates were identified by 16S rRNA gene sequence analysis, and the key players are shown in Figure 4. Species closely related to *Scytonema hyalinum* (Fig. 4c), *Nostoc* sp. (Fig. 4h), or *Trichocoleus sociatus*, *Pseudophormidium* sp. (Fig. 4g) and *P. minor* (Fig. 4d) were shared across most sites (Table 2). Cyanobacterial species that were unique for lithic microhabitats included *Alteriella* sp. (Fig. 4a), *Gloeocapsopsis* sp. (Fig. 4e), and *Kastovskya adunca* (Fig. 4b), whereas others such as *Phormidesmis* sp., *Nodosolinea epilithica*, and *Mojavia pulchra* only occurred in soils. Green algae were identified in soil samples by Baumann et al. (2018), but here we also identified a minor proportion of lithic green algae, most of which could be assigned to members of the genera *Stichococcus*, *Chlorella*, *Trebouxia*, *Spongiocloris*, *Aptatococcus*, and *Myrmecia* (data not shown).

The PA core site contained the species poorest communities with five edaphic species and five hypolithic species of which two were shared between sites (Fig. 5a). Most species were found at the site SG with 11 edaphic species and seven hypolithic species of which five species were shared between sites (Fig. 5d). At the PA core site, the hypolithic limestone and chasmoendolithic granite cyanobacterial communities differed strongly from the edaphic community (Fig. 5, b and c). Beta-diversity ordination showed highest similarities between the edaphic and lithic communities from the site SG and indicated a strong divergence at the site PA core between the two hypolithic sites and the edaphic sites as well as the chasmoendolithic site (Fig. 5e).

**Phylogeny.** A total of 44 partial 16S rRNA gene sequences (390 bp) were obtained from all samples processed, and all of these exhibited a similarity >97% compared to sequences published in GenBank (NCBI-NIH), so that a robust phylogenetic tree could be constructed based on cyanobacteria of the Atacama Desert (Fig. 6). Most of the taxa were identified to the genus and some to the species level, such as *Trichocoleus desertorum* ATA2-1-CV7, *Pseudophormidium* sp. ATA2-1-KO12, *Nostoc* sp. ATA2-1-CV6, or *Kastovskya adunca* ATA6-11RM11.

K ( $g \cdot kg^{-1}$ )	Mg ( $g \cdot kg^{-1}$ )	Mn ( $mg \cdot kg^{-1}$ )	P ( $mg \cdot kg^{-1}$ )	Zn ( $mg \cdot kg^{-1}$ )	pH (H <sub>2</sub> O)	EC (mS $\cdot$ cm <sup>-1</sup> )
5.62 ± 0.90 <sup>b</sup>	7.88 ± 4.52	1104.09 ± 259.09	367.76 ± 88.48 <sup>a</sup>	54.33 ± 7.20 <sup>b</sup>	6.51 ± 0.18 <sup>a</sup>	1688.00 ± 919.92
1.93 ± 0.44 <sup>a</sup>	1.51 ± 0.46	183.24 ± 42.95	260.78 ± 71.73 <sup>a</sup>	31.21 ± 21.90 <sup>ab</sup>	7.93 ± 0.14 <sup>c</sup>	2724.33 ± 1925.64
1.71 ± 0.76 <sup>a</sup>	1.01 ± 1.35	255.26 ± 265.39	185.31 ± 233.75 <sup>a</sup>	15.25 ± 14.34 <sup>a</sup>	7.13 ± 0.18 <sup>b</sup>	317.00 ± 400.91
2.00 ± 0.27 <sup>ab</sup>	2.55 ± 0.23	316.09 ± 69.69	699.20 ± 85.82 <sup>b</sup>	22.54 ± 7.96 <sup>a</sup>	8.06 ± 0.32 <sup>c</sup>	50.33 ± 12.58

## DISCUSSION

Here, we show that cyanobacterial species richness decreases with decreasing water availability, confirming our first hypothesis that only tolerant species can cope with high xeric stress under low water conditions. Also, in accordance with our second hypothesis, the divergence of soil- (edaphic) and stone (lithic)-inhabiting cyanobacterial communities increased with decreasing water availability. In the following sections the two hypotheses are discussed based on the comparisons between PA and SG and on comparisons between the three sites of PA (ridge, grit, core).

*Effects of different water sources on edaphic and lithic cyanobacterial communities.* Increasing levels of rainfall from PA (long term mean annual rainfall  $15 \text{ mm} \cdot \text{y}^{-1}$ ) to SG (long-term mean annual rainfall  $83 \text{ mm} \cdot \text{y}^{-1}$ ) result in a greater cyanobacterial species richness in edaphic communities at SG. This increased richness can be explained by the fact that cyanobacteria require liquid water to be photosynthetically active, since they are unable to use other water sources such as high air humidity (Lange et al. 1986, Büdel and Lange 1991). Besides precipitation, soil properties such as a thicker A horizon and more P in SG soils (Table 1) may have not only led to higher levels of vegetation (Bernhard et al. 2018), greater abundances of bacterial and archaeal 16S rRNA gene copy numbers (Oeser et al. 2018), but also to a higher cyanobacterial species richness. This may be explained by a broader ecological niche at SG compared with the more arid site of PA, which provides more favorable conditions for the establishment of edaphic cyanobacterial species. The broader ecological niche at SG does not only favor a greater species richness but also leads to a higher congruence between edaphic and lithic communities since specialization toward xeric stress is less important (Fig. 5).

Lithic cyanobacterial species richness was likely higher at PA because low cloud frequency was higher (32%) compared with SG (18%; Baumann et al. 2018). This implies a higher fog water availability at PA. Azúa-Bustos et al. (2011) has shown that more fog water condensed at cooler quartz stones, which in turn, and in addition to rainfall, is accessible to hypolithic communities. For these reasons it could be assumed that cyanobacteria at SG depend less on the lithic habitat compared with the more diverse lithic community at arid PA.

Similar effects of the source of water on lithic and edaphic communities were observed for the W-E gradient in PA. Stomeo et al. (2013) also found that hypolithic communities exhibited a fog-related distribution along a W-E aridity gradient in the Namib Desert. Water availability and different soil types form a gradient at PA: on the one hand, fog and dew are the main drivers for life (Lehnert et al. 2018) together with rare rainfall events. Here, a

gradient is formed where total precipitation decreases from the coast ( $110 \text{ mm} \cdot \text{y}^{-1}$ ) to the inland ( $17 \text{ mm} \cdot \text{y}^{-1}$ ). On the other hand, there are different types of substrates along this gradient ranging from silt- and clay-rich soil at the site PA ridge close to the Pacific Ocean to granite and quartz grit ( $>5 \text{ mm}$ ) at the site PA grit and non-weathered porous granite rocks at the site PA core (Fig. 1, c–e). In addition to the limitations caused by soil structure and fog water availability, other soil parameters, such as nitrogen and phosphorus, seem to play a role because they were found to be similar in PA ridge, PA grit, and PA core (Table 1). Therefore, the increased xeric stress caused by less precipitations in this transect determined a decrease in total species richness (Fig. 5a; Table 2), thus supporting hypothesis (i).

Further inland, at the PA grit site, the highest congruence (70%) between lithic and edaphic cyanobacteria was found (Fig. 5a), which may be due to the similar structure of the soil substrate (grit) and the bigger quartz stones that were colonized by biofilms. At PA core, 60% of all observed species had a distinct habitat (Fig. 5a) and the nMDS showed the strongest divergence between the lithic and edaphic communities as well as among the lithic communities (chasmoendolithic and hypolithic) for all sites (Fig. 5e). While hypolithically colonized quartz and limestones only showed minor differences within the community composition (Fig. 5e), the chasmoendolithic microhabitats of cracks and fissures of granitoid stones and rocks strongly differed. Diruggiero et al. (2013) also reported chasmoendolithic communities from the Atacama Desert that were dominated by *Chroococcidiopsis* species, together with only one phylotype that could be assigned to the order Nostocales, which was reflected here by the detection of *Scytonema hyalinum* (Nostocales; Fig. 4c) as the only filamentous species for the chasmoendolithic PA core site. By comparing PA ridge with PA core the divergence between lithic and edaphic communities can be seen to increase with increasing xeric stress from the coast toward the inland of PA (Fig. 5a), thus confirming hypothesis (ii).

*In situ detection of lithic cyanobacterial communities.* Whenever different substrates such as stones or complex soil structures are colonized by cyanobacteria, it is crucial to visualize the phototrophs' interaction with these substrates in order to better understand their localization and ecological niche. This has been repeatedly applied to lithic communities from hot and dry deserts (Azúa-Bustos et al. 2011, Yung et al. 2014, Gómez-Silva 2018). In the present study, bright field, FEI, and CLSM allowed for a preliminary inspection of the cyanobacterial community (Fig. 3). These methodologies are useful tools whenever a first overview of cyanobacterial community present in terrestrial biofilms is required and can also provide observations based on

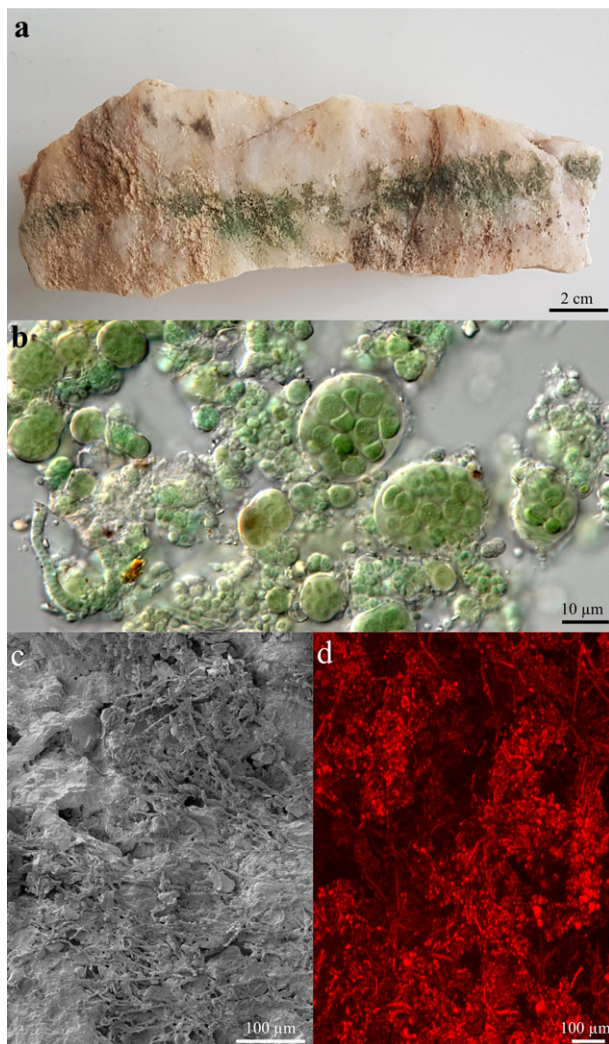


FIG. 3. Microscopy of hypolithic biofilms. (a) Quartz stone with hypolithic biofilm from PA ridge. (b) Bright field microscopy of biofilm scraped off the stone surface. (c) In situ FEI microscopy of air-dried biofilm samples showing a matrix of mineral particles and filamentous cyanobacteria. (d) In situ CLSM image of wetted biofilm samples showing filamentous and coccoidal cyanobacteria. [Color figure can be viewed at [wileyonlinelibrary.com](http://wileyonlinelibrary.com)]

morphological details of individual microorganisms. Compared with findings of De los Ríos et al. (2006, 2014), who reported structural differences within moss and/or cyanobacterial dominated biofilms of endo-/hypolithically colonized granite from continental Antarctica, we generally also found a dense matrix of cyanobacteria, extracellular polysaccharides, and mineral particles (Fig. 3c). While De los Ríos et al. (2006, 2014) identified only one unspecified cyanobacterial strain, we found a matrix that was formed by several filamentous cyanobacteria such as *Pseudophormidium* sp. and single-celled species like *Pleurocapsa minor* and *Chroococcidiopsis* sp. (Fig. 4b). Interestingly, a strong dominance of filamentous taxa was detected when FEI was applied to air-dried in situ samples from more humid sites

(Fig. 3c). Additionally, collapsed coccoidal species, which were less visible than filamentous cyanobacteria and thus more difficult to differentiate were detected from these sites. In contrast, hypolithic and chasmoendolithic microhabitats of the dry site PA core appeared to be dominated by unicellular species such as *Chroococcidiopsis*. Similar trends have previously been reported for the Atacama Desert (Azúa-Bustos et al. 2011, Yung et al. 2014, Gómez-Silva 2018), which implies that among coccoid genera, such as *Chroococcidiopsis*, *Pleurocapsa*, and *Gloeocapsopsis*, highly specialized species exist that are highly adapted to the lithic microhabitat. In the present study, CLSM (used on stone attached wet biofilms) was found to be a better technique for reflecting the cyanobacterial community due to a less disturbed overview of the community. CLSM images clearly indicated a similar proportion of single-celled cyanobacteria with filamentous species (Fig. 3d), which could be confirmed by light microscopy of the biofilm (Fig. 3b). Accordingly, the CLSM technique seems to be the method of choice when comparing the properties of different morphological groups of cyanobacteria in situ.

*Assignment of cyanobacterial species to edaphic and lithic habitats.* In general, our results suggest that some species, such as *Gloeocapsopsis* sp. (Fig. 4e), conform to the concept of strictly lithic or edaphic cyanobacteria. This species showed high similarities to other species of its genus isolated from the Atacama Desert (Fig. 6; *Gloeocapsopsis* sp. AAB1), that have been found on quartz stones biosynthesizing sucrose and trehalose in response to desiccation (Azúa-Bustos et al. 2014).

In addition, we found three species of cyanobacteria only in soils (*Phormidesmis* sp., *Nodosolinea epilithica*, *Mojavia pulchra*), while other species were solely present in lithic habitats (*Aliterella* sp., *Gloeocapsopsis* sp., *Kastovskya adunca*). In contrast to our results, *Kastovskya adunca* (Fig. 4b) has been found in both habitats (Schwabe 1960, Mühlsteinova et al. 2014) preventing a clear assignment of this species to a distinct microhabitat. A similar case may apply to the recent assigned genus *Aliterella* (Fig. 4a). A few known species have been isolated from soil and sea water (Rigonato et al. 2016), but the strain isolated by us from the Atacama Desert appears to be a new species based on the investigated gene fragment (Fig. 6). This suggests that species of the genus *Aliterella* still cannot be the strictly assigned to either lithic or edaphic habitats. Our results, like Makhallanyane et al. (2013) who investigated hypolithic cyanobacteria in the Namib Desert, provide strong evidences for a high congruence between lithic and edaphic cyanobacterial communities in the Atacama Desert and also the existence of some few specialists for each niche. Makhallanyane et al. (2013) concluded that hypolithons do not develop independently from microbial communities found in the surrounding soil, but selectively recruit from local populations and also



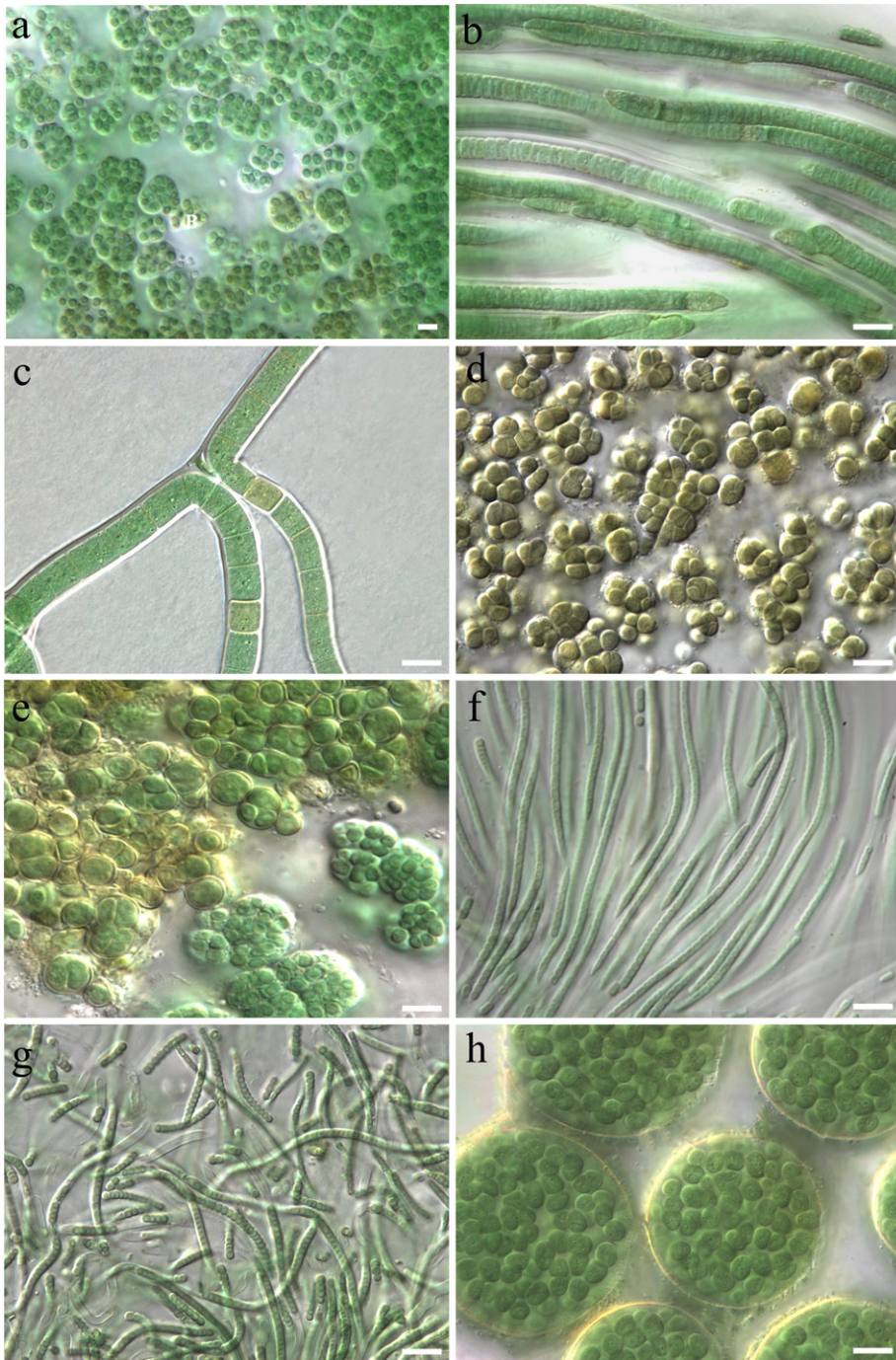


FIG. 4. Bright field microscopy of cyanobacterial isolates. (a) *Aliterella* sp., (b) *Kastovskya adunca*, (c) *Scytonema hyalinum*, (d) *Pleurocapsa minor*, (e) *Gloeocapsopsis* sp., (f) *Trichocoleus desertorum*, (g) *Pseudophormidium* sp., and (h) *Nostoc* sp. Scale bars indicate 10  $\mu\text{m}$ . [Color figure can be viewed at [wileyonlinelibrary.com](http://wileyonlinelibrary.com)] ]

from the existence of a few specialists in each niche (Makhalanyane et al. 2013).

This study shows a strong consistency between the taxonomic assignments attained from the direct microscopy observation of the samples, the microscopy observation of the isolates obtained, and their phylogenetic analyses. Furthermore, sequences obtained from isolates of this study such as those from *Trichocoleus sociatus*, some *Nostoc* sp., *T. desertorum*, *Kastovskya adunca*, *Gloeocapsopsis* sp., and *Pseudophormidium* sp., could even be assigned to

sequences obtained from taxa isolated from the Atacama Desert during previous studies (Fig. 6; for example, accession abbreviation ATA). This validates the applied polyphasic approach that combines morphological and phylogenetic results.

#### SUMMARY

Sequencing and microscopy allowed us to inspect the edaphic and lithic cyanobacterial communities present at the southern edge of the Atacama Desert.

TABLE 2. List of species detected by 16S rDNA gene sequences and bright field microscopy ( $n = 5$ ). X represents the presence of species.

Type Substrate Location	Soil community				Hypolithic					Chasmo-endolithic Granite PA core	
	Soil				Quartz				Limestone PA core		
	PA ridge	PA grit	PA core	SG	PA ridge	PA grit	PA core	SG			
<i>Aliterella</i> sp.											x
<i>Chroococidiopsis</i> sp.	x	x	x			x	x		x		x
<i>Gloeocapsopsis</i> sp.						x	x		x		
<i>Kastovskya adunca</i>						x			x		
<i>Leptolyngbya</i> sp.				x		x					
<i>Microcoleus vaginatus</i>		x	x	x	x						
<i>Mojavia pulchra</i>	x										
<i>Myxosarcina</i> sp.		x				x					
<i>Nodosolinea epilithica</i>				x							
<i>Nostoc</i> cf. <i>edaphicum</i>		x		x				x			
<i>Nostoc</i> cf. <i>punctiforme</i>				x				x			
<i>Nostoc</i> sp.	x	x	x	x	x	x	x	x	x		
<i>Phormidesmis</i> sp.	x			x							
<i>Phormidium autumnale</i>		x		x	x	x					
<i>Pleurocapsa minor</i>		x	x		x	x					x
<i>Pseudophormidium</i> sp.	x				x			x	x		
<i>Scytonema hyalinum</i>		x			x	x		x			x
<i>Tolypothrix</i> sp.		x				x					
<i>Trichocoleus badius</i>			x	x				x			
<i>Trichocoleus desertorum</i>				x	x			x			
<i>Trichocoleus sociatus</i>	x	x		x	x			x			x
Species richness	6	10	5	11	8	10	5	7	5		5

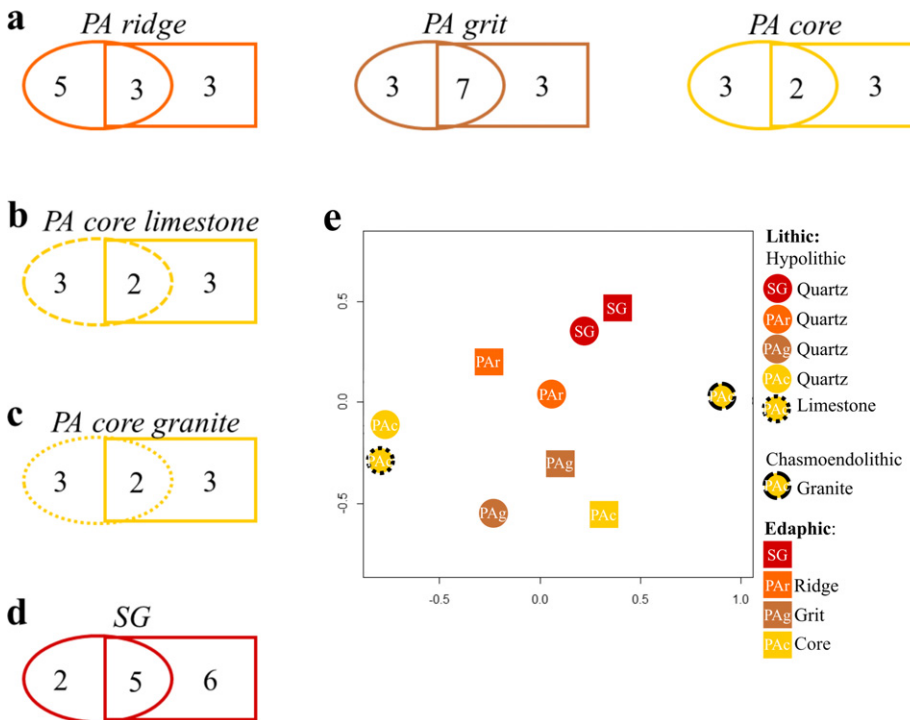


FIG. 5. Venn diagrams of cyanobacterial communities. Venn diagrams (a–d) for species in edaphic microenvironments (rectangles) and lithic microenvironments (circles). The number of species shared is shown in the overlapping areas. (a) Hypolithic quartz community compared to edaphic community of the same habitat along the W-E precipitation gradient of PA. (b) Hypolithic limestone community compared to edaphic community. (c) Chasmoendolithic community compared to edaphic community. (d) Hypolithic quartz community compared to edaphic community. (e) Beta-diversity nMDS ordination of the similarity in cyanobacterial community composition of different sites and substrates (stress = 0.13). [Color figure can be viewed at [wileyonlinelibrary.com](http://wileyonlinelibrary.com)]

A total of 21 cyanobacterial species were identified. In combination with soil and climate data, a decrease in species richness along a N-S gradient along the Coastal Cordillera and the declining water availability along a W-E precipitation gradient of the Atacama Desert was observed. In these arid ecosystems, lithic microhabitats such as translucent quartz stones are considered to be refugia for

cyanobacterial communities. Our analyses suggest that the composition of both edaphic and lithic communities diverge as xeric stress increases. Higher precipitation resulted in edaphic and lithic communities showing high congruence compared to arid conditions where only a few species were shared between both microhabitats, resulting in more distinct communities.

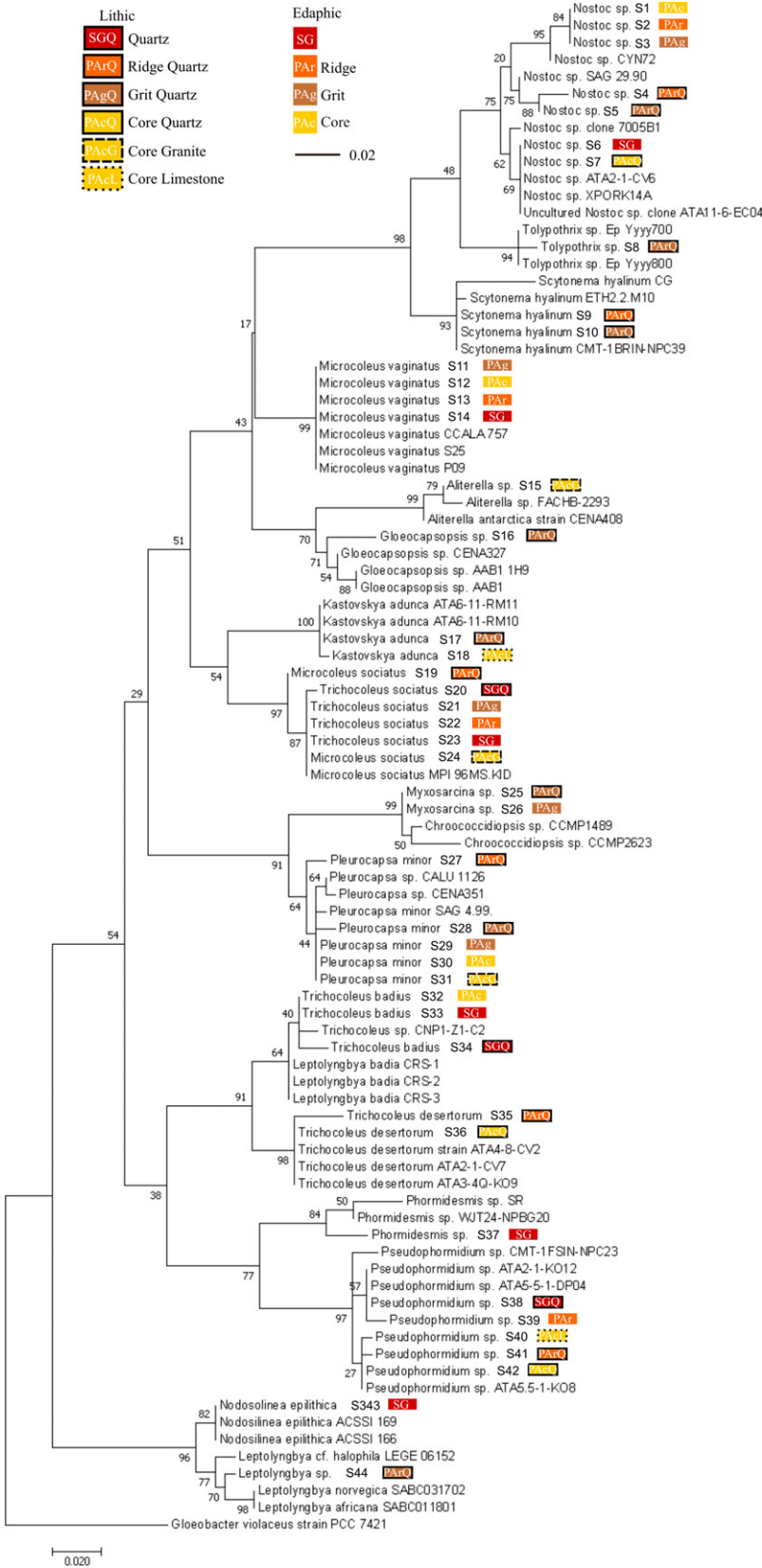


FIG. 6. Phylogenetic tree. Maximum likelihood phylogenetic tree obtained from the aligned a 16S rRNA gene sequences. Color and abbreviation codes denote the origin of the isolates, sites, and type of substrates. [Color figure can be viewed at wileyonlinelibrary.com]

The authors thank Dr. Karin Glaser, University of Rostock, for guidance through statistical analysis and Dr. Thomas Löber, University of Kaiserslautern, for taking the FEI images at the NSC (Nano Structuring Center) as well as Dorothea Siebel for her help during the sequencing process. Additionally, we want to thank the Corporación Nacional Forestal (CONAF), Chile, for their support during field work and Dr. Kirstin Übernickel, University of Tübingen for providing precipitation data. The sites *SG* and *PA core* are study sites of the priority program *Earth-Shape* (“Earth Surface Shaping by Biota”) funded by the German Research Foundation.

#### DATA ACCESSIBILITY STATEMENT

Sequences can be found in the European Nucleotide Archive (ENA) under the project code PRJEB31521.

#### CONFLICT OF INTEREST

The authors have no conflict of interest to report.

- Adriaenssens, E. M., Van Zyl, L., De Maayer, P., Rubagotti, E., Rybicki, E., Tuffin, M. & Cowan, D. A. 2015. Metagenomic analysis of the viral community in Namib Desert hypoliths. *Environ. Microbiol.* 17:480–95.
- Anderson, M. J. 2001. A new method for non-parametric multivariate analysis of variance. *Aust. Ecol.* 26:32–46.
- Azúa-Bustos, A., González-Silva, C., Mancilla, R. A., Salas, L., Gómez-Silva, B., McKay, C. P. & Vicuña, R. 2011. Hypolithic cyanobacteria supported mainly by fog in the coastal range of the Atacama Desert. *Microb. Ecol.* 61:568–81.
- Azúa-Bustos, A., Urrejola, C. & Vicuña, R. 2012. Life at the dry edge: microorganisms of the Atacama Desert. *FEBS Lett.* 586:2939–45.
- Azua-Bustos, A., Zúñiga, J., Arenas-Fajardo, C., Orellana, M., Salas, L. & Rafael, V. 2014. *Gloeocapsopsis* AAB1, an extremely desiccation-tolerant cyanobacterium isolated from the Atacama Desert. *Extremophiles* 18:61–74.
- Baumann, K., Jung, P., Samolov, E., Lehnert, L. W., Büdel, B., Karsten, U., Bendix, J. et al. 2018. Biological soil crusts along a climatic gradient in Chile: richness and function of phototrophic microorganisms in phosphorus biogeochemical cycling. *Soil Biol. Biochem.* 127:286–300.
- Bernhard, N., Moskwa, L. M., Schmidt, K., Oeser, R. A., Aburto, F., Bader, M. Y., Baumann, K. et al. 2018. Pedogenic and microbial interrelations to regional climate and local topography: new insights from a climate gradient (arid to humid) along the Coastal Cordillera of Chile. *Catena* 170:335–55.
- Bischof, H. & Bold, H. 1963. Some soil algae from enchanted rock and related algal species. *University of Texas Publications*, Austin, TX, USA 6318:1–95.
- Blume, H. P., Stahr, K. & Leinweber, P. 2011. *Bodenkundliches Praktikum*, 3rd edn. Spektrum Akademischer Verlag, Heidelberg, p 255.
- Bozkurt, D., Rondanelli, R., Garreaud, R. & Arriagada, A. 2016. Impact of warmer eastern tropical Pacific SST on the March 2015 Atacama floods. *Mon. Weather Rev.* 144:4441–60.
- Bray, J. R. & Curtis, J. T. 1957. An ordination of the upland forest communities of southern Wisconsin. *Ecol. Monogr.* 27:325–49.
- Büdel, B. & Lange, O. L. 1991. Water status of green and blue-green phycobionts in lichen thalli after hydration by water vapor uptake: Do they become turgid? *Bot. Acta.* 104:361–6.
- Chen, M. & Ma, L. Q. 2001. Comparison of three aqua regia digestion methods for twenty Florida soils. *Soil Sci. Soc. Am. J.* 65:491–9.
- Christian, K., Kaestli, M. & Gibb, K. 2017. Spatial patterns of hypolithic cyanobacterial diversity in Northern Australia. *Ecol. Evol.* 7:7023–33.
- De los Ríos, A., Cary, C. & Cowan, D. 2014. The spatial structures of hypolithic communities in the Dry Valleys of East Antarctica. *Polar Biol.* 37:1823–33.
- De los Ríos, A., Grube, M., Sancho, L. G. & Ascaso, C. 2006. Ultrastructural and genetic characteristics of endolithic cyanobacterial biofilms colonizing Antarctic granite rocks. *FEMS Microbiol. Ecol.* 59:386–95.
- Diruggiero, J., Wierzcchos, J., Robinson, C. K., Souterre, T., Ravel, J., Artieda, O. & Ascaso, C. 2013. Microbial colonisation of chasmoendolithic habitats in the hyper-arid zone of the Atacama Desert. *Biogeosciences* 10:2439–50.
- Falconer, R. E. & Falconer, P. D. 1980. Determination of cloud water acidity at a mountain observatory in the Adirondack Mountains of New York State. *J. Geophys. Res. Oceans* 85:7465–70.
- Geitler, L. 1932. *Cyanophyceae von Europa unter Berücksichtigung der anderen Kontinente*. Akademische Verlagsgesellschaft, Leipzig.
- Gómez-Silva, B. 2018. Lithobiontic life: “Atacama rocks are well and alive”. *A. Van Leeuw. J. Microb.* 111:1333–1343.
- Gorbushina, A. A. 2007. Life on the rocks. *Environ. Microbiol.* 9:1613–31.
- Johansen, J. R., Kovacic, L., Casamatta, D. A., Iková, K. F. & Kaštovský, J. 2011. Utility of 16S-23S ITS sequence and secondary structure for recognition of intrageneric and intergeneric limits within cyanobacterial taxa: *Leptolyngbya corticola* sp. nov. (Pseudanabaenaceae, Cyanobacteria). *Nova Hedwigia* 92:283–302.
- Jukes, T. H., Cantor, C. R. & Munro, H. N. 1969. Evolution of protein molecules. *Mamm. Protein Metab.* 3:132.
- Jung, P., Briegel-Williams, L., Simon, A., Thyssen, A. & Büdel, B. 2018a. Uncovering biological soil crusts: carbon content and structure of intact Arctic, Antarctic and alpine biological soil crusts. *Biogeosciences* 15:1149–60.
- Jung, P., Schermer, M., Briegel-Williams, L. & Büdel, B. 2018b. Strong in combination: Polyphasic approach enhances arguments for cold-assigned endemism. *Microbiologyopen*. 8:E00729.
- Komárek, J. & Anagnostidis, K. 1998. *Cyanoprokaryota, Vol. 1, Chroococcales*. Süßwasserflora von Mitteleuropa, Springer Publishing, Weisbaden, Germany, p. 759.
- Komárek, J. & Anagnostidis, K. 2005. *Süßwasserflora von Mitteleuropa, 2. Teil/end Part: Oscillatoriales*. Springer, Weisbaden, Germany, p 759.
- Kumar, S., Stecher, G. & Tamura, K. 2016. MEGA7: Molecular Evolutionary Genetics Analysis version 7.0 for bigger datasets. *Mol. Biol. Evol.* 33:1870–4.
- Lange, O. L., Kilian, E. & Ziegler, H. 1986. Water vapor uptake and photosynthesis of lichens: performance differences in species with green and blue-green algae as phycobionts. *Oecologia* 71:104–10.
- Langhans, T. M., Storm, C. & Schwabe, A. 2009. Community assembly of biological soil crusts of different successional stages in a temperate sand ecosystem, as assessed by direct determination and enrichment techniques. *Microb. Ecol.* 58:394–407.
- Le, P. T., Makhalanyane, T. P., Guerrero, L. D., Vikram, S., Van de Peer, Y. & Cowan, D. A. 2016. Comparative metagenomic analysis reveals mechanisms for stress response in hypoliths from extreme hyperarid deserts. *Genome Biol. Evol.* 8:2737–47.
- Lehnert, L. W., Thies, B., Trachte, K., Achilles, S., Osses, P., Baumann, K., Jung, P. & Karsten, U. 2018. A case study on fog/low stratus occurrence at Las Lomitas, Atacama Desert (Chile) as a water source for biological soil crusts. *Aerosol Air Qual. Res.* 18:254–69.
- Makhalanyane, T. P., Valverde, A., Lacap, D. C., Pointing, S. B., Tuffin, M. I. & Cowan, D. A. 2013. Evidence of species recruitment and development of hot desert hypolithic communities. *Env. Microbiol. Rep.* 5:219–24.

- Mühling, M., Woolven-Allen, J., Murrell, J. C. & Joint, I. 2008. Improved group-specific PCR primers for denaturing gradient gel electrophoresis analysis of the genetic diversity of complex microbial communities. *ISME J.* 2:379.
- Mühlsteinova, R., Johansen, J. R., Pietrasiak, N., Martin, M. P., Osorio-Santos, K. & Warren, S. D. 2014. Polyphasic characterization of *Trichocoleus desertorum* sp. nov. (Pseudanabaenales, Cyanobacteria) from desert soils and phylogenetic placement of the genus *Trichocoleus*. *Phytotaxa* 163:241–61.
- Oeser, R. A., Stroncik, N., Moskwa, L. M., Bernhard, N., Schaller, M., Canessa, R. & Fuentes, J. P. 2018. Chemistry and microbiology of the Critical Zone along a steep climate and vegetation gradient in the Chilean Coastal Cordillera. *Catena* 170:183–203.
- Pointing, S. B. & Belnap, J. 2012. Microbial colonization and controls in dryland systems. *Nat. Rev. Microbiol.* 10:551–62.
- Pointing, S. B., Chan, Y., Lacap, D. C., Lau, M. C., Jurgens, J. A. & Farrell, R. L. 2009. Highly specialized microbial diversity in hyper-arid polar desert. *Proceedings of the National Academy of Sciences* 106(47):19964–19969.
- R Development Core Team 2017. *R: A Language and Environment for Statistical Computing*. R Foundation for Statistical Computing, Vienna, Austria.
- Rigonato, J., Gama, W. A., Alvarenga, D. O., Branco, L. H. Z., Brandini, F. P., Genuário, D. B. & Fiore, M. F. 2016. *Aliterella atlantica* gen. nov., sp. nov., and *Aliterella antarctica* sp. nov., novel members of coccoid Cyanobacteria. *Int. J. Syst. Evol. Micr.* 66:2853–61.
- Rundel, P., Dillon, M. O., Palma, B., Mooney, H. A., Gulmon, S. L. & Ehleringer, J. R. 1990. The phylogeography and ecology of the coastal Atacama and Peruvian deserts. *Aliso* 13:1–50.
- Schulze-Makuch, D., Wagner, D., Kounaves, S. P., Mangelsdorf, K., Devine, K. G., de Vera, J. P. & Galy, A. 2018. Transitory microbial habitat in the hyperarid Atacama Desert. *Proc. Natl. Acad. Sci. USA* 115:2670–5.
- Schwabe, G. H. 1960. Zur autotrophen Vegetation in ariden Böden. Blaualgen und Lebensraum IV. *Osterreichische Botanische Zeitschrift* 107:281–309.
- Stanier, R. Y., Kunisawa, R., Mandel, M. & Cohen-Bazire, G. 1971. Purification and properties of unicellular blue-green algae (Order Chroococcales). *Bacteriol. Rev.* 35:171–205.
- Thomas, D. N. 2005. Photosynthetic microbes in freezing deserts. *Trends Microbiol.* 13:87–8.
- Tracy, C. R., Streten-Joyce, C., Dalton, R., Nussear, K. E., Gibb, K. S. & Christian, K. A. 2010. Microclimate and limits to photosynthesis in a diverse community of hypolithic cyanobacteria in northern Australia. *Environ. Microbiol.* 12:592–607.
- Van Goethem, M. W., Makhalyanyane, T. P., Valverde, A., Cary, S. C. & Cowan, D. A. 2016. Characterization of bacterial communities in lithobionts and soil niches from Victoria Valley, Antarctica. *FEMS Microbiol. Ecol.* 92:fiw051.
- Vogel, S. 1955. Niedere “Fensterpflanzen” in der sudafrikanischen wüste. *Beitr. Biol. Pflanz.* 31:45–135.
- Warren-Rhodes, K. A., Rhodes, K. L., Boyle, L. N., Pointing, S. B., Chen, Y., Liu, S., Zhuo, P. & McKay, C. P. 2007. Cyanobacterial ecology across environmental gradients and spatial scales in China’s hot and cold deserts. *FEMS Microbiol. Ecol.* 61:470–82.
- Wierzos, J., De los Rios, A. & Ascaso, C. 2013. Microorganisms in desert rocks: the edge of life on earth. *Int. Microbiol.* 15:171–81.
- Williams, L., Jung, P., Zheng, L. J., Maier, S., Peer, T., Grube, M. & Büdel, B. 2018. Assessing recovery of biological soil crusts across a latitudinal gradient in Western Europe. *Restoration Ecology* 26(3):543–554.
- Yung, C. C., Chan, Y., Lacap, D. C., Pérez-Ortega, S., de los Rios-Murillo, A., Lee, C. K. & Pointing, S. B. 2014. Characterization of chasmoendolithic community in Miers Valley, mcmurdo Dry Valleys, Antarctica. *Microb. Ecol.* 68:351–9.